Environ Monit Assess (2017) 189: 349
DOI 10.1007/s10661-017-6033-0

Eco-friendly synthesis of silver nanoparticles using green algae (*Caulerpa serrulata*): reaction optimization, catalytic and antibacterial activities

Eman F. Aboelfetoh · Rania A. El-Shenody · Mohamed M. Ghobara

Received: 15 October 2016 / Accepted: 30 May 2017 / Published online: 23 June 2017

Abstract Stable colloidal silver nanoparticles (AgNPs) were synthesized using *Caulerpa serrulata* (green marine algae) aqueous extract as an efficient reducing and stabilizing agent. This method is considered to be a sustainable alternate to the more complicated chemical procedures. To achieve the optimization synthesis of AgNPs, several effects such as extract concentration, contact time, pH values, and temperature were examined. The synthesized AgNPs were characterized by UV–Vis spectroscopy, FT-IR, XRD, and HR-TEM. The synthesized AgNPs showed an intense surface plasmon resonance band at 412 nm at the optimal conditions (20% (v/v) extract and 95 °C). TEM reveal that higher extract concentration and higher temperature leading to the formation of spherical AgNPs with an average particle size of 10 ± 2 nm. The synthesized AgNPs showed excellent catalytic reduction activity of Congo red (CR) dye from aqueous solutions. The degradation percentage of CR with AgNPs accelerated by increasing either $NaBH_4$ concentration or catalytic dosage. The AgNPs synthesized at higher temperature (e.g., 10Ag-95) exhibited the highest catalytic activity. The reaction kinetics was found to be pseudo first order with respect to the dye concentration. Moreover, the AgNPs displayed antibacterial activity at lower concentration against *Staphylococcus aureus*, *Pseudomonas aeruginosa*, *Shigella* sp., *Salmonella typhi*, and *Escherichia coli* and may be a good alternative therapeutic approach. The outcomes of the current study confirmed that the synthesized AgNPs had an awesome guarantee for application in catalysis and wastewater treatment.

Keywords AgNPs · Marine algae · Optimization · Catalyst · Kinetics · Antibacterial

E. F. Aboelfetoh (✉)
Chemistry Department, Faculty of Science, Tanta University, Tanta, Egypt
e-mail: eman.fahmy@science.tanta.edu.eg
R. A. El-Shenody · M. M. Ghobara
Botany Department, Faculty of Science, Tanta University, Tanta, Egypt

Introduction

Metal nanoparticles assume a crucial role in a large number of applications as they show superior physicochemical properties (optical, catalytic activity, magnetic, electronic, and antibacterial properties) due to their significantly small size and very high surface/volume ratio (Indana et al. 2016; Pandey and Ramontja 2016). The extremely small size of these metal nanoparticles presents a very high reactive surface area that add to their significant enhancement in the properties in comparison to their pure metal counterparts (Indana et al. 2016). The greatly small size of nanoparticles, particularly in the case of silver nanoparticles (AgNPs), finds their utility in various applications such as biomedical, healthcare, pharmaceutical, cosmetics, environmental, catalysis, hardware, water treatment, and energy (Abbasi et al. 2016; Gangula et al. 2011; Liu et al. 2015, 2017b; Liu and Astruc 2017; Ngo et al. 2012; Priyadarshini et al. 2014; Tiwari et al. 2010; Wang et al. 2017).

AgNPs can be manufactured by several methods such as chemical reduction, electrochemical techniques, photochemical reduction, sonochemical, microwave, γ-radiation and laser ablation (Gabriel et al. 2017; Gurusamy et al. 2017; Khan et al. 2011; Liu et al. 2017a; Pal et al. 2009; Rajabi et al. 2017; Verma et al. 2017; Zhang et al. 2017). Unfortunately, the chemical reduction method which is commonly used for preparing AgNPs is still expensive and employ hazardous organic solvents and toxic reducing agents (Gurusamy et al. 2017; Loo et al. 2012). Additionally, it is usually required the presence of a stabilizing agent to avoid excessive aggregation of the formed nanoparticles (Khodashenas and Ghorbani 2015; Ren et al. 2015). Therefore, there has been a growing necessity to substitute the chemical synthetic procedures with eco-friendly systems.

Currently, the use of green chemistry to protect our global environment is getting to be focal issues in many fields of research. Therefore, there is a significant concern in the development of environmental and sustainable methods for the synthesis of nanoparticles. Green synthesis of metal nanoparticles using extracts of natural products is a promising innovation that would beat the obstructions in chemical methods indicated so far. Different biological processes have been reported for the synthesis of metal nanoparticles using various plant extract, honey, bacteria, and fungi (Ahmed et al. 2016; Dong et al. 2017; Indana et al. 2016; Kathiraven et al. 2015; Khalil et al. 2014; Loo et al. 2012; Narayanan et al. 2015; Philip 2010).

Plant metabolites including sugars, terpenoids, polyphenols, alkaloids, phenolic acids, and proteins act as reducing and capping agents for the nanoparticles (Makarov et al. 2014). These biomolecules contain various functional groups capable of nanoparticle formation. Therefore, the resulted nanoparticles are protected from further reactions and aggregation, which increases their stability (Makarov et al. 2014). It was found that the concentration and compositions of these biological active components control the size and morphology of the resulted nanoparticles. Recent studies have revealed that several forms of marine algae have the ability to produce a variety of nanoparticles (El-Kassas and Ghobrial 2017; Fawcett et al. 2017; González-Ballesteros et al. 2017). In general, algae are assorted into three groups in perspective of the algal body or thallus pigmentation. The color groups are green algae (chlorophytes), red algae (rhodophytes), and brown algae (phaeophytes) (Fawcett et al. 2017; Kim 2011). Marine plants contain a wide assortment of biologically active compounds and secondary metabolites that empower these plants to act as biological factories for the production of metal and metal oxide nanoparticles (Rajakumar and Rahuman 2016). *Caulerpa serrulata* is a type of green marine algae belongs to Caulerpaceae. *Caulerpa* are particularly well known in the Indo-Pacific region. Some species of this genus are mainly used as a human food in the form of fresh vegetables owing to their delicious taste and their nutritional properties. Caulerpa contains proteins, minerals, fiber, polyunsaturated fatty acids, vitamins, and bioactive antioxidants (de Gaillande et al. 2016a, b; Nagappan and Vairappan 2014). Caulerpenyne and caulerpin, the most abundant metabolites of Caulerpa, exhibited powerful antimicrobial activity against human pathogenic bacteria and antitumor activities for several human cancer cell lines (Barbier et al. 2001; Fischel et al. 1994; Nagappan and Vairappan 2014; Sfecci et al. 2017). The measure of such items changes among species and between various seasons (de Gaillande et al. 2016; Dumay et al. 2002). The synthesis of AgNPs via the extract of other Caulerpa species (*Caulerpa racemose*) is preformed (Edison et al. 2016a; Kathiraven et al. 2015). For our knowledge, there is no published study dealing with the synthesis of AgNPs utilizing *C. serrulata*.

The control of water pollution is a challenging task for researchers around the globe. The major contribution to water pollution is by dyeing industries. Congo red dye—a synthetic azo dye—is broadly used as colorant in several industrial fields such as textile, leather, paper mill, printing, and cosmetic industries (Saratale et al. 2011; Shah et al. 2016). The removal of azo dyes including Congo red from discharged sewage remains of a great concern due to their carcinogenicity, mutagenicity, and non-degradability (Priyadarshini et al. 2014; Shah et al. 2016; Wang et al. 2013).Various techniques have been employed for the removal of dyes and contaminants from wastewaters, such as coagulation, oxidation, membrane separation, adsorption, photocatalytic degradation, and reduction degradation (Aboubaraka et al. 2017; Ayati et al. 2014; Garcia et al. 2013; Gemeay et al. 2017; Nesic et al. 2016; Yian Zheng 2012). Reduction degradation may come to be a new category of dye wastewater treatment way, since it may arrange monstrous volume and innumerable concentrations of color wastewater (Chen et al. 2014; Ghosh et al. 2015; Nasrollahzadeh et al. 2016).

The current study aims to contribute to the development of a green, simple, and inexpensive method to eliminate the toxic dyes from ecosystem. Therefore, we investigate the eco-friendly synthesis of AgNPs using *C. serrulata* (green marine algae) aqueous extract for the first time, for our knowledge, as a reducing agent and an efficient stabilizer instead of using harmful reductant and expensive stabilizing agents such as surfactants and polymers. The impact of various parameters on the synthesis process is studied to achieve the optimum conditions. The potential application of the synthesized nanoparticles was tested in the removal efficiency of azo dye (Congo red) from aqueous solution. In addition, the antibacterial activity of the synthesized AgNPs has been investigated.

Experimental

C. serrulata algae extraction

C. serrulata (Fig. 1) was collected from the Red Sea coast, Egypt (26° 45′ N, 33° 57′ E). After cleaning and drying at room temperature, it was grounded into powder. About 1 g of algae powder was heated in 100 mL of de-ionized water at 70 °C for 10 mins. The unrefined extract was filtrated and the filtrate kept in fridge (4 °C).

Synthesis of AgNPs

Typically, a certain volume of the *C. serrulata* extract (5–25) mL was added to 10^{-3} M of $AgNO_3$ solution and the volume was adjusted to 100 mL with de-ionized water. The reduction process of Ag^+ to Ag^0 nanoparticles was associated with color change of the solution from yellow to reddish brown depending on different parameters such as the extract volume, stirring time, temperature, and pH values. The pH of the solutions is adjusted using 0.1 M HCl or 0.1 M NaOH solutions. The synthesis of AgNPs was estimated by UV–Visible measurements of the mixture through the reaction. The biosynthesized AgNPs were characterized by HRTEM, XRD, and FT-IR spectroscopy. Table 1 shows the synthesis conditions and the abbreviation symbols of all synthesized AgNPs samples.

Fig. 1 Photograph of *Caulerpa serrulata* (green marine algae)

The catalytic activity assessment

To assess the catalytic properties of the synthesized AgNPs, the reduction of azo dye (CR) as biorefractory and carcinogenic pollutants in the presence of $NaBH_4$ was selected as a model reaction. Briefly, 3 mL of $NaBH_4$ solution (1.74 mM) was mixed well with CR aqueous solution (0.067 mM). To this solution, certain volume of the synthesized AgNPs was added. Keep the total volume of the main solution at 10 mL. UV–Vis spectrophotometer was used to monitor the progress of the reaction at regular time intervals in a scanning range 350–650 nm at room temperature. In aqueous medium, CR dye shows maximum absorption band at 498 nm.

The antibacterial test

The antibacterial activity of AgNPs were investigated using *Escherichia coli*, *Staphylococcus aureus*, *Shigella* sp., and *Salmonella typhi* (gram negative bacteria) and *Pseudomonas aeruginosa* (gram positive bacteria). The minimal inhibition concentration (MIC) of AgNPs for each test microorganism was determined by applying agar well diffusion technique (Ashokkumar et al. 2015). About 50 μL of extract was used as negative control in all experiments. Approximately, 20 mL of sterilized and cooled Müller Hinton agar medium was poured into sterilized Petri dishes and allowed to solidify at room temperature. The overnight growth test organisms were transferred and spread over the agar medium using a sterile cotton swab for each test microorganism, and then wells were made. After that, different concentrations of colloidal AgNPs (25, 50, and 75 μL) were added to the wells. The AgNPs inoculated plates were incubated at 37 °C for 24 h. After incubation, the zone of inhibition around the well was measured. All the experiments were followed three times for statistical analysis.

Table 1 The synthesis conditions of AgNPs samples after 24 h and the catalytic reduction of CR dye (0.067 mM) by the synthesized AgNPs under different conditions

Synthesis conditions			Catalytic reduction conditions					
Samples	Extract conc. (v/v) %	Temp (°C)	Degradation (%)	Time (min)	$NaBH_4$ conc. (mM)	AgNPs dosage (mL)	Rate const. (min^{-1})	R^2
5Ag	5	27	76.2	20	1.74	0.10	0.06	0.999
10Ag	10	27	90.5	20	1.74	0.10	0.08	0.997
20Ag	20	27	96.0	16	1.74	0.10	0.13	0.994
10Ag-95	10	95	99.3	12	1.74	0.10	0.21	0.995
20Ag-95	20	95	84.9	20	1.74	0.10	0.07	0.998
20Ag	20	27	96.0	16	1.74	0.10	0.13	0.997
20Ag	20	27	99.0	13	3.15	0.10	0.21	0.998
20Ag	20	27	99.0	08	4.91	0.10	0.46	0.998
20Ag	20	27	99.7	05	5.71	0.10	0.58	0.999
20Ag	20	27	96.0	16	1.74	0.10	0.13	0.994
20Ag	20	27	99.0	12	1.74	0.20	0.26	0.994
20Ag	20	27	99.0	09	1.74	0.25	0.34	0.994
20Ag	20	27	99.0	06	1.74	0.30	0.46	0.995

Characterization of AgNPs

The UV–Visible spectra of AgNPs were recorded using Cary 400 UV–Visible Spectrophotometer at a resolution of 0.5 nm. XRD pattern was done by MXP-18 (Mac science Co. Ltd) diffractometer with Cukα radiation. FT-IR estimations were completed using PerkinElmer 1430 by employing KBr pellet system. The morphology, size distribution, and Lattice structure of AgNPs were examined by high-resolution transmission electron microscope (HR-TEM), JEM-2100. The electron diffraction design for a chose zone was additionally recorded. ^{1}H and ^{13}C NMR spectra were measured by a Bruker DRX-400 spectrometer operating at 400 MHz (in DMSO-d6) with chemical shifts stated as ppm.

Results and discussion

UV–Visible analysis of AgNPs

Noble metal nanoparticles (plasmonic) are distinguished from other nanoparticles such as semiconductor quantum dots, polymeric, and magnetic nanoparticles by their unique surface plasmon resonance (SPR). Optical absorption spectra of AgNPs is dominated by SPR which illustrates a shift toward the red or blue end depends on particle size, state of aggregation, shape, and the surrounding dielectric medium (Mahmudin et al. 2015). The synthesis of AgNPs was monitored by color change and UV–Vis spectroscopy. The formation of AgNPs was confirmed by changing in the solution color from pale yellow to reddish brown. To achieve the optimum conditions for the synthesis of AgNPs, different factors were studied in this procedure such as the extract concentration, stirring time, pH, and temperature.

Effect of extract concentration

The effect of *C. serrulata* extract concentration on the synthesis of AgNPs was studied by adding different extract concentrations (5–25%) to 10^{-3} M $AgNO_3$ solution at room temperature (27 °C) after 24 h. The intensity of the SPR bands increased and shifted to lower wavelength (435 nm) while increasing the concentration of the extract from 5 to 20% (Fig. 2a). This blue shift demonstrates a decrease in AgNPs mean diameter (Khalil et al. 2014). Further increase of the extract concentration (25%) reduces the intensity of the SPR band. This is perhaps because of the aggregation of nanoparticles, which is in concurrence with previous study (Velammal et al. 2016).

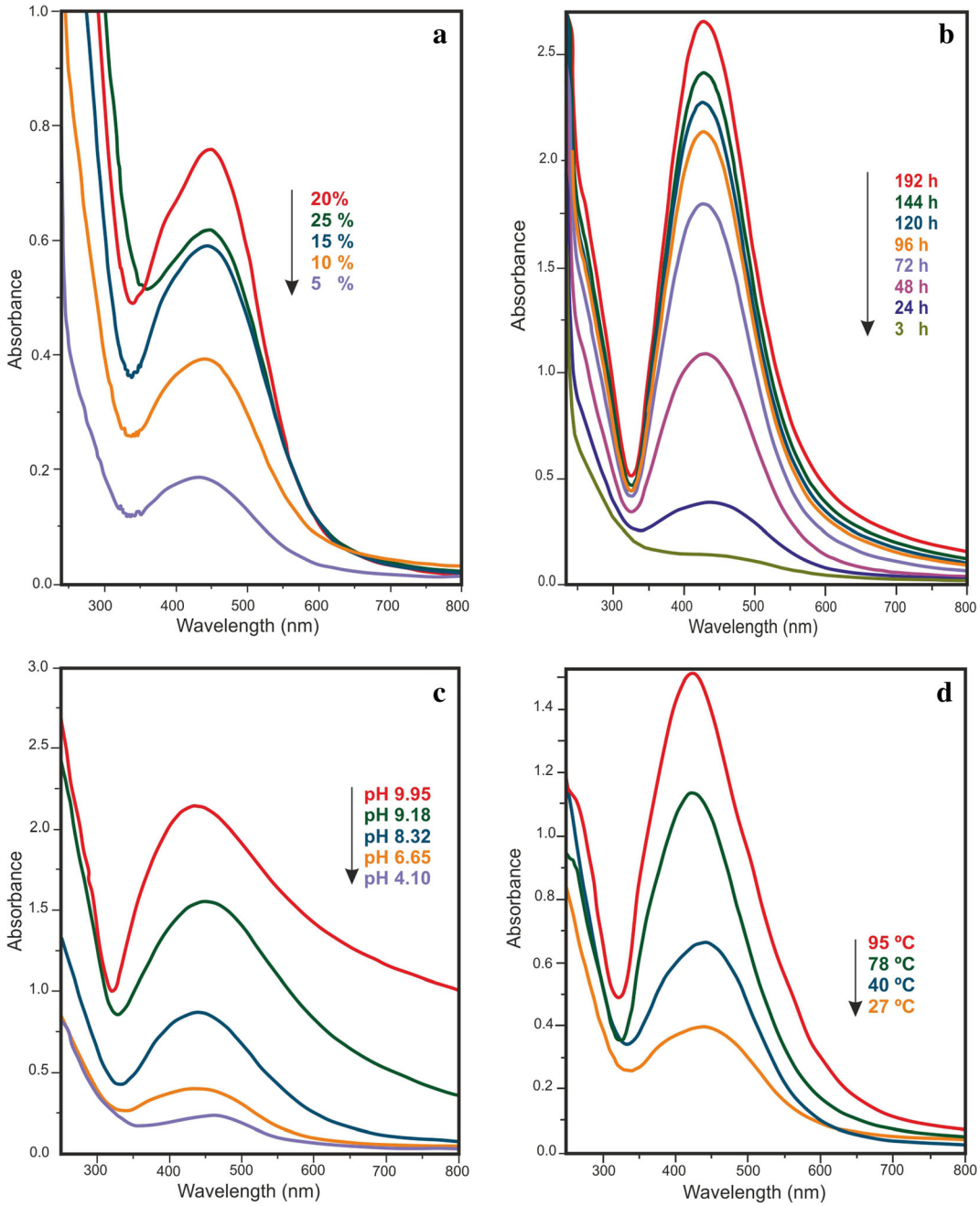

Fig. 2 UV–Vis spectra of AgNPs formed using 10^{-3} M $AgNO_3$ after 24 h at 27 °C with **a** various extract conc. (v/v%), **b** 10% extract as a function of contact time, **c** 10% extract at diverse pH values and **d** 10% extract at diverse temperatures

Effect of contact time

The reaction between silver ions and the reducing materials in the extract was followed during 8 days at room temperature. Figure 2b shows the UV–Visible spectra of AgNPs as a function of time after addition of 10% extract. Increasing the contact time resulted in increasing the intensity of the SPR band, with no shift and thus a rapid increase in the number of AgNPs. This result implies that the AgNPs prepared by this method is very stable without aggregation. Amazingly, after 5 months, AgNPs still stable and no precipitation occurs.

Effect of pH

It was observed that the color of reaction mixture and the intensity of the SPR bands were pH-dependent. The effect of different pH values on the synthesis process of AgNPs was studied (Fig. 2c). In the alkaline medium, the reducing and stabilizing ability of *C. serrulata* extract is enhanced. While increasing the pH values from 6.65 to 9.95, the absorbance was increased and a narrow SPR band at lower wavelength was noticed (427 nm). At low pH (4.10), the solution color was turned into dark red quickly and a broad band at higher wavelength (470 nm) was detected. The appearance of this broad band reflected the aggregation of AgNPs. In agreement, previous studies reported the acid medium enhance the formation of AgNPs with large particle size, whereas in alkaline medium, the AgNPs was formed with small size (Loo et al. 2012; Siddiqui et al. 2017). The present investigation indicates the formation of large number of AgNPs with smaller diameter at higher pH values.

Effect of temperature

It is apparent from Fig. 2d that the temperature highly affect the synthesis process of the AgNPs. At lower temperature (27 °C), the formation of AgNPs was associated with appearance of light yellow color and less intense SPR band at higher wavelength (440 nm). As the reaction temperature increases from 27 to 95 °C, the slow reduction rate of silver ions is enhanced and the characteristic band for AgNPs was significant after 1 h. At higher temperature (95 °C), UV–Vis spectra show sharp intense SPR band at lower wavelength (412 nm), which clearly indicates the formation of smaller AgNPs. In agreement with previously published article, as the temperature was increased, the reactants were consumed rapidly leading to the formation of smaller nanoparticles (Ibrahim 2015). Moreover, at 95 °C, the intensity of SPR band was significantly increased by increasing the extract concentration to 20% (not shown). The AgNPs formed at 95 °C by using 10 and 20% extract were assigned as 10Ag-95 and 20Ag-95 respectively (Table 1).

FT-IR analysis

FT-IR measurements were recorded to identify the major functional groups on the *C. serrulata* to examine their possible involvement in the production and capping of AgNPs. FT-IR spectrum of *C. serrulata* aqueous extract shows different bands positioned at 3429, 2929, 2859, 1730, 1638, 1428, 1379, 1242, 1147, 1034, and 741 cm^{-1} (Fig. 3a). The presence of bands at 3447 and 1730 cm^{-1} could be related to stretching of (O–H) and C=O groups respectively. Small bands positioned at 2929 and 2859 cm^{-1} may be due to (C-H) stretching of alkanes. A sharp intense band observed at 1613 cm^{-1} can be due to the stretching vibration of alkene C=C group. The observed band at 1194, 1125, and 1023 are due to C–O stretching vibration. Small bands at 2300–2336 cm^{-1} may indicate the presence of C≡C stretching (Yian Zheng 2012). The main bands existing in the extract are also present in FT-IR spectrum of the synthesized AgNPs with lower intensities and slight shift (Fig. 3a). This strongly recommends that the extract act not only as bioreductant, but also act as stabilizers on the surface of the AgNPs. This may indicate that the extract acted as bioreductant and stabilizer.

^{13}C NMR and ^{1}H NMR analysis

In agreement with FT-IR, ^{13}C NMR confirm the existence of aliphatic carbon at 39.3–40.8 ppm, C=C carbon at 61 ppm and C≡C carbon at 70–73 ppm (Fig. 3b). The C=O of acetoxy group appeared at 101 ppm (Pretsch et al. 2000). Furthermore, the ^{1}H NMR support the previous data (Fig. 3c). The more shielded protons of CH_3, CH_2 indicate the presence of peaks at high field 0.84–1.85 ppm, the proton of CH_3 of acetoxy group appeared at 2.1–2.9 ppm. The peak at 8.3 ppm refers to the existence of OH, while the peak at 4.3–5.59 reflect the presence of olefinic C-H (Pretsch et al. 2000). Previous study revealed that the main constituents present in the organic extract of *Caulerpa* (green marine algae) are caulerpenyne and caulerpin (Ciavatta et al. 2006; Marić et al. 2017; Wells et al. 2016). Based on our NMR and FT-IR analysis, we could expect that caulerpenyne and/or its derivatives (Fig. 4) are the possible constituents of aqueous extract of *C. serrulata* responsible for the bioreduction of silver ions.

XRD analysis

The XRD patterns (Fig. 3d) show the distinctive diffraction peaks of AgNPs at 2θ = 38.13°, 44.31°, 65.16° and 77.25°, which matches to the (111), (200), (220), and

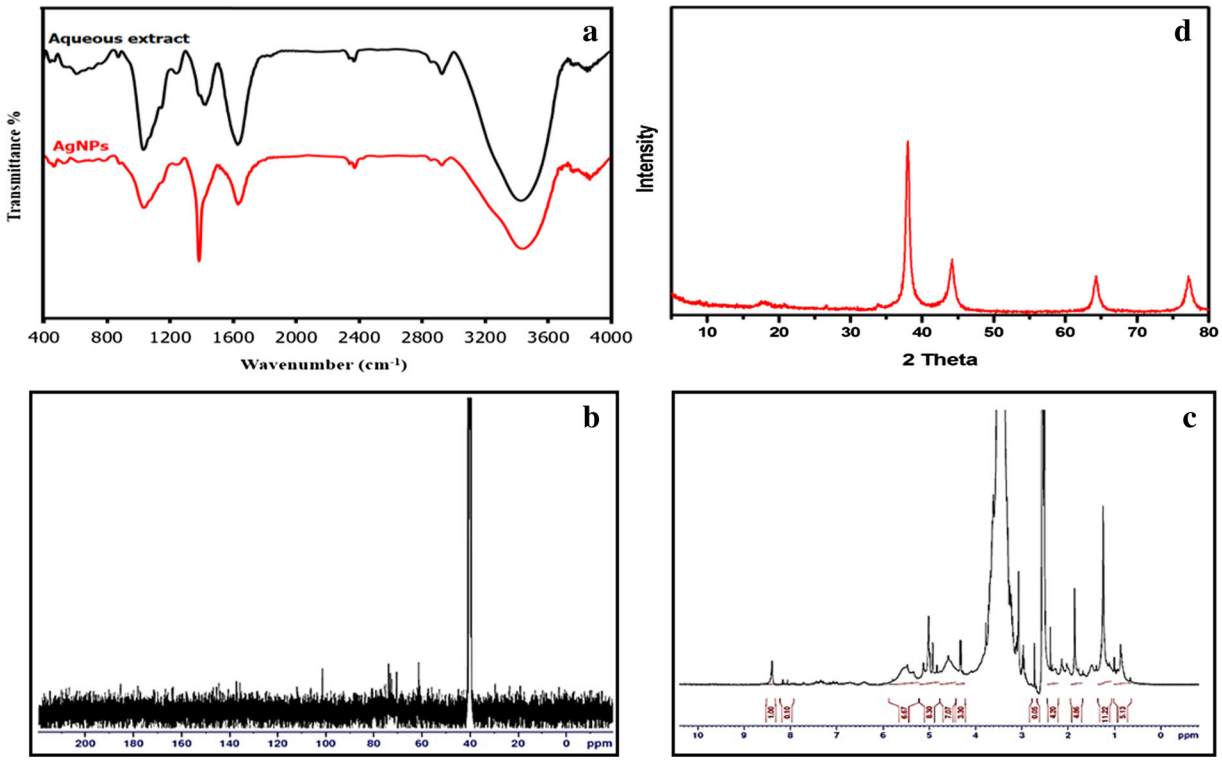

Fig. 3 **a** FT-IR spectra of *C. serrulata* extract and AgNPs, **b**, **c** ^{13}C NMR and ^{1}H NMR of extract in deuterated DMSO and **d** XRD pattern of AgNPs

(311) lattice planes of face centered cubic crystal structure (Ashokkumar et al. 2015).

HR-TEM analysis

In order to acquire more information about the shape and size of the synthesized AgNPs, HR-TEM analysis was employed. It can be noted that the extract concentration highly effect not only the shape of nanoparticles but also their sizes. At 95 °C and at lower extract concentration (10%), the AgNPs possess mainly spherical and ellipsoidal shapes beside minor amounts of silver nanocubic and nanorods (Fig. 5a–c). As the extract concentration increases to 20% at the same temperature, the AgNPs were exhibited mainly the spherical shape structure and the particle size decreased as shown in (Fig. 5d, e). Moreover, the average particle size distribution reflects the obvious reduction of AgNPs size as the

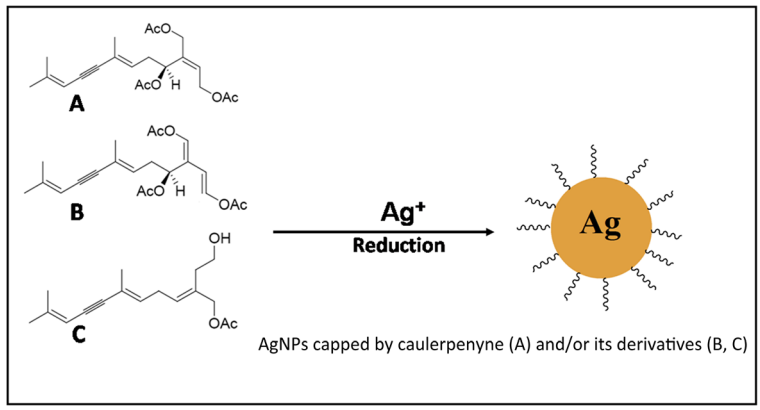

Fig. 4 Possible chemical constituents of aqueous extract of *C. serrulata* responsible for the reduction of silver ions, where *A* refers to the caulerpenyne and *B*, *C* denotes its derivatives (Ciavatta et al. 2006; Sfecci et al. 2017)

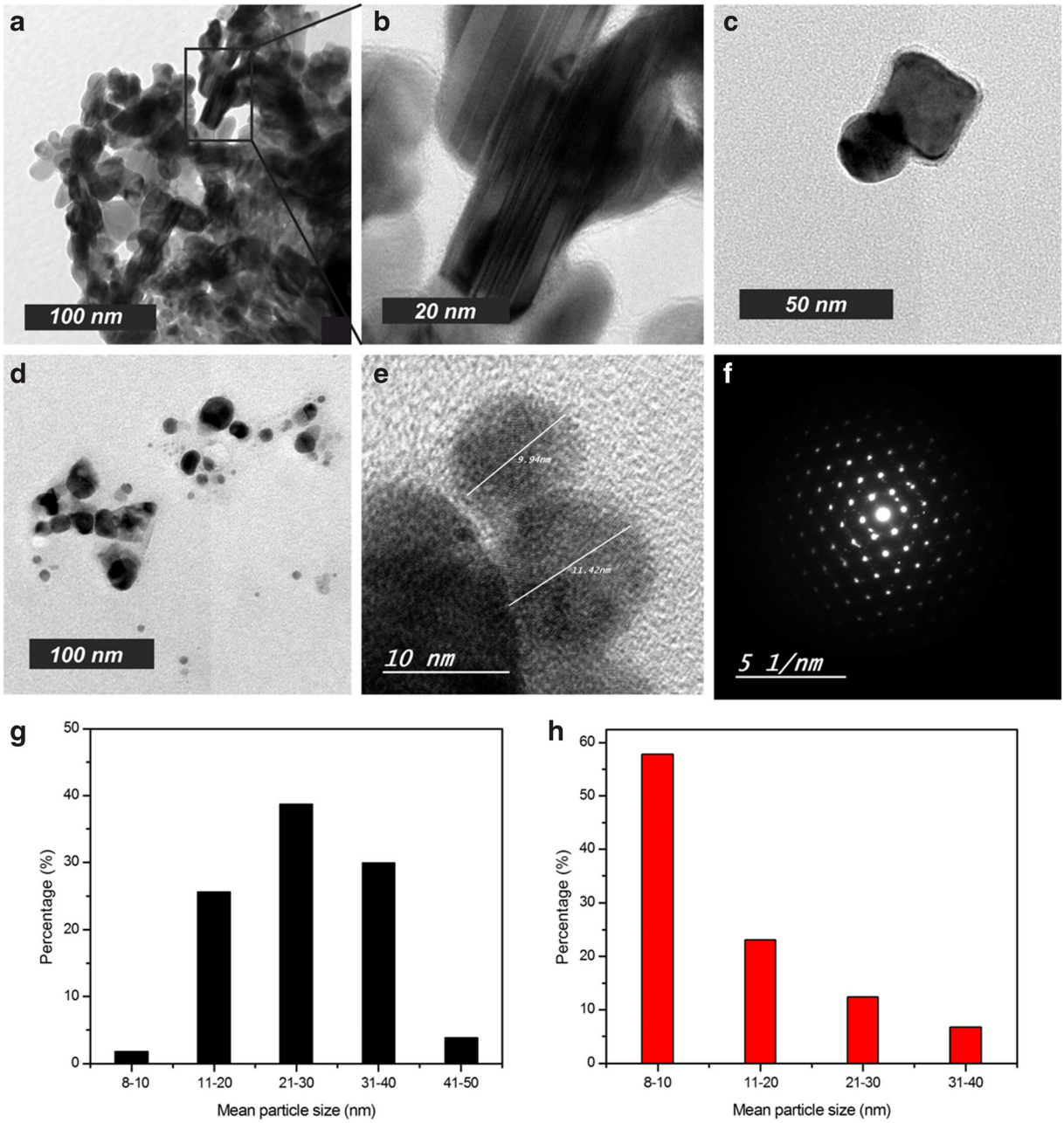

Fig. 5 TEM images of AgNPs (**a**–**e**), SAED image (**f**) and particle size distribution of AgNPs synthesized at 95 °C for 24 h using 10% and 20% extract respectively (**g**, **h**)

extract concentration increases, where at 20% extract, smaller particles with an average size of 10 ± 2 nm was more pronounced (Fig. 5g, h). This could be due to an increase of capping layer around the synthesized AgNPs. Additionally, the selected area electron diffraction (SAED) image reflects the crystalline nature of AgNPs (Fig. 5f).

The catalytic activity of the synthesized AgNPs

The catalytic performance of the biosynthesized AgNPs was assessed in the reduction of aqueous solution of CR dye in the presence of sodium borohydride ($NaBH_4$) at room temperature. The color of CR solution with an excess of $NaBH_4$ remained unchanged for 3 h (Fig. 6a),

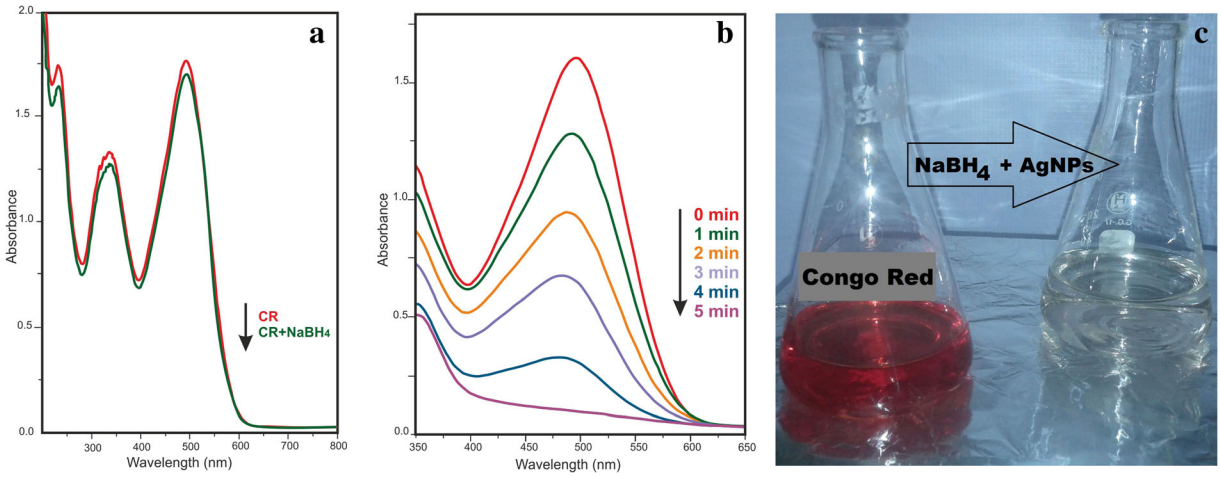

Fig. 6 **a** UV–Vis spectra of CR (0.072 mM) using $NaBH_4$ (3.15 mM) in the absence of AgNPs after 3 h, **b** After adding 0.20 mL of AgNPs (20Ag), and **c** Photograph of the decolorization of CR dye

indicating that the reduction frequency was negligible in the absence of the AgNPs. However, as soon as the biosynthesized AgNPs is added into the reaction medium, the color of CR disappeared within 5 mins (Fig. 6b, c), signifying the excellent catalytic activity of AgNPs for the reduction of CR.

Effect of extract concentration

We have studied the catalytic degradation of CR using various AgNPs synthesized at two different temperatures (27 °C and 95 °C) using different extract concentrations (5%, 10% and 20%). The information acquired from the catalytic reduction tests were then used to estimate the reduction degradation percentage (%) of the CR by the following equation:

$$Degradation\% = \frac{A_0 - A_t}{A_0} \cdot 100$$

Where A_0 is the initial absorbance of CR and A_t is the absorbance of CR after certain time intervals. It is obvious from Fig. 7a that the reduction percentage of CR by the AgNPs synthesized at room temperature (27 °C) increased with the increase in the extract concentration according the following order 5Ag > 10Ag > 20Ag. This might reflect the increase in the quantity of AgNPs in that direction (Fig. 2a). Interestingly, the reduction rate of the AgNPs synthesized at 95 °C using 10% extract concentration (10Ag-95) showed higher activity than that synthesized at room temperature (10Ag). The observed increase in activity could be attributed to the significant increase in the number of AgNPs at higher temperature. On the other hand, at higher temperature, (95 ºC) increasing the extract concentration to 20% as with sample (20Ag-95) leads to significant decrease in the catalytic activity. This could be due to the smaller size of AgNPs as confirmed by TEM and also the increase in the surface coverage by the biomolecules. Such increased coverage hinders the diffusion of CR on the AgNPs surface (Gangula et al. 2011).

Effect of $NaBH_4$ concentration

The concentration of $NaBH_4$ deeply affects the catalytic reduction percentage of CR. Figure 7b shows the Degradation percentage of CR with different concentrations of $NaBH_4$ (1.71–5.71 mM) using 10Ag as a catalyst. The reduction percentage of CR with 10Ag accelerated with the rise in the $NaBH_4$ concentration. The best degradation rate attained when the concentration of $NaBH_4$ was 85 equivalent to CR concentration. The linear relationship between ln (A_t/A_0) and the reduction time (min) (Fig. 8a) shows that the reduction degradation of CR follows the pseudo first-order kinetics. This is because the initial concentration of $NaBH_4$ was higher than that of CR, therefore it remained essentially constant throughout the reaction. The reaction rate constants were estimated from the slopes of the graphs and recorded with the corresponding correlation coefficients (Table 1).

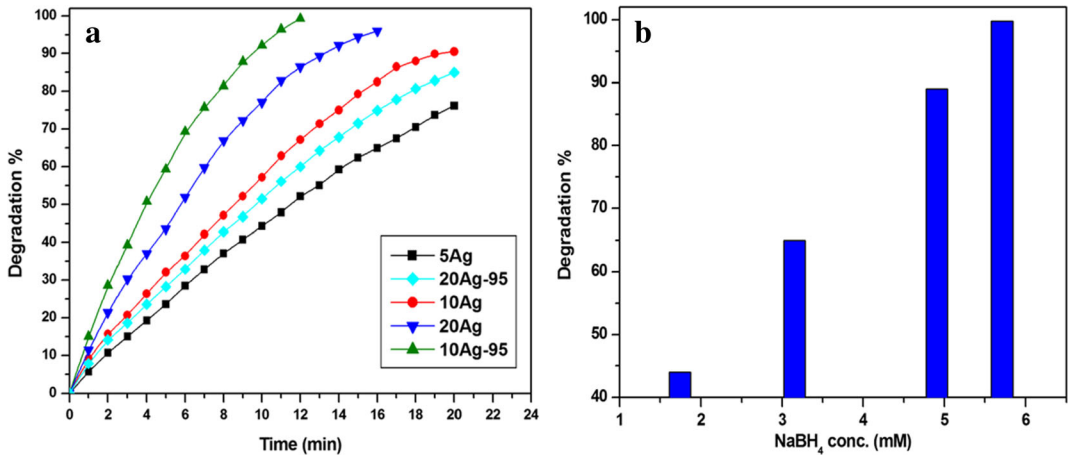

Fig. 7 **a** Degradation % of CR (0.067 mM) with $NaBH_4$ (1.74 mM) and 0.1 mL of AgNPs (5Ag, 10Ag, 20Ag, 10Ag-95, and 20Ag-95) and **b** Degradation % of CR (0.067 mM) with various conc. of $NaBH_4$ and 0.1 mL of AgNPs (20Ag) after 5 mins

Effect of the catalyst dosage

In order to study the effect of the catalytic dosage on the degradation percentage of CR, the reaction was performed with varying volumes of the AgNPs in the presence of constant concentration of $NaBH_4$ (1.74 mM) and CR (0.067 mM). As illustrated in Fig. 8b, the rate of degradation increases with the increase in the catalytic dosage from 0.1 to 0.3 mL. This could be due to the availability of active sites on the catalyst surface. The rate constants obtained from the kinetic data for all the synthesized samples were shown in Table 1. Compared with other catalysts in the reported literatures, the synthesized AgNPs displayed excellent catalytic performance and exhibited higher rate constants (Table 2).

The catalytic reduction of CR by the synthesized AgNPs (Scheme 1) could be clarified by Langmuir-Hinshelwood model. In view of this model, both of the reactants (CR and $NaBH_4$) were initially adsorbed on the AgNPs surface and afterward $NaBH_4$ gives the electrons to AgNPs; further, the AgNPs exchange these electrons to CR (acceptor), achieving the debilitating of the azo double bond by means of conjugation. The reduction of CR happens at the surface of AgNPs by conveying electrons from the donor BH_4^- to CR. In this reaction, $NaBH_4$ acts as electron donor and hydrogen supplier (Khodadadi et al. 2017; Sreekanth et al. 2016; Vidhu and Philip 2014). As a result of the large surface area of the AgNPs as well as its high negative potential (−1.80 V vs NHE), it acts as electron transfer mediator

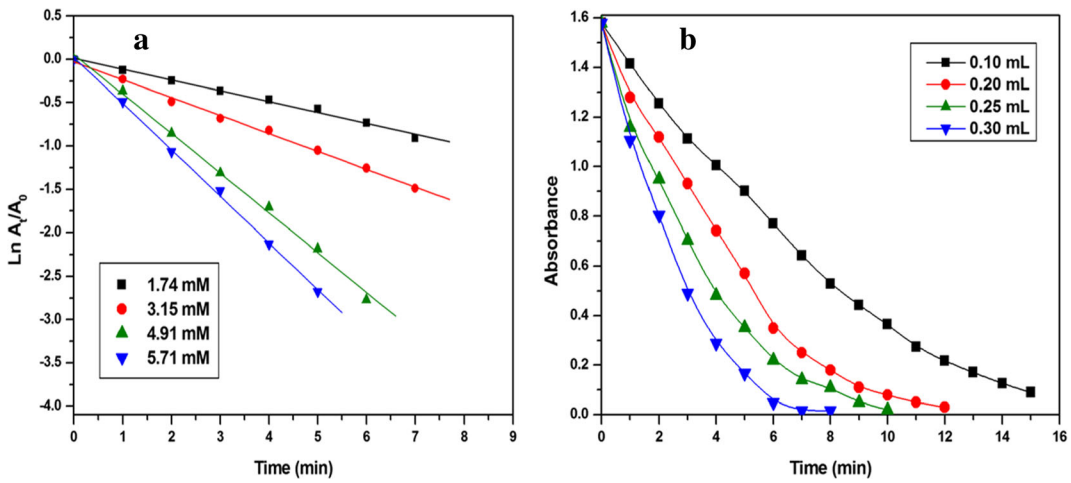

Fig. 8 **a** Pseudo first-order kinetics plots of the degradation of CR (0.067 mM) with various conc. of $NaBH_4$ and 0.1 mL of 20Ag and **b** The decrease in absorbance of CR (0.067 mM) versus time in the presence of $NaBH_4$ (1.74 mM) and different dosages of AgNPs (20Ag)

Table 2 Comparison of various catalysts in the reduction of CR dye with $NaBH_4$

Catalysts	$NaBH_4$ (mM)	CR conc. (mM)	Rate constant (min^{-1})	References
AuNPs	150	1	0.219	(Nadaf and Kanase 2016)
AgNPs	10	1	0.148	(Indana et al. 2016)
AgNPs/polymer microgel	–	–	0.201	(Shah et al. 2016)
AuNPs/polymer microgel	–	–	0.375	(Shah et al. 2016)
Cu^0/chitosan-cellulose microfibers	100	0.012	0.165	(Kamal et al. 2016)
AuNPs	10	1	0.236	(Ganapuram et al. 2015)
Cu^0/SPA-15	25	0.020	0.600	(Ghosh et al. 2015)
AgNPs (20Ag)	5.71	0.067	0.580	This work

between BH_4^- and CR and thus showing higher degradation efficiency for the dye (Edison et al. 2016b).

Antibacterial activity of the synthesized AgNPs

The results of antibacterial activity of AgNPs were shown in Figs. 9 and 10. The antibacterial activity was found to be straightly reliant on the concentration of the AgNPs. The maximum inhibition zone was found in *E. coli* (21 mm for 75 μL) and the minimum inhibition zone was found in *S. typhi* (10 mm for 50 μL). Results dissimilarity might be due to different interactions of AgNPs with the tested organisms and also due to the susceptibility of the organism used in the current study. The main mechanism of AgNPs toxicity probably related to the attachment of AgNPs to the negatively charged bacterial cell wall, where they can disrupt its shape and permeability of the plasma membrane. Also, all studies had confirmed that silver ions released from nanoparticle surface contribute to their toxicity. Both AgNPs and

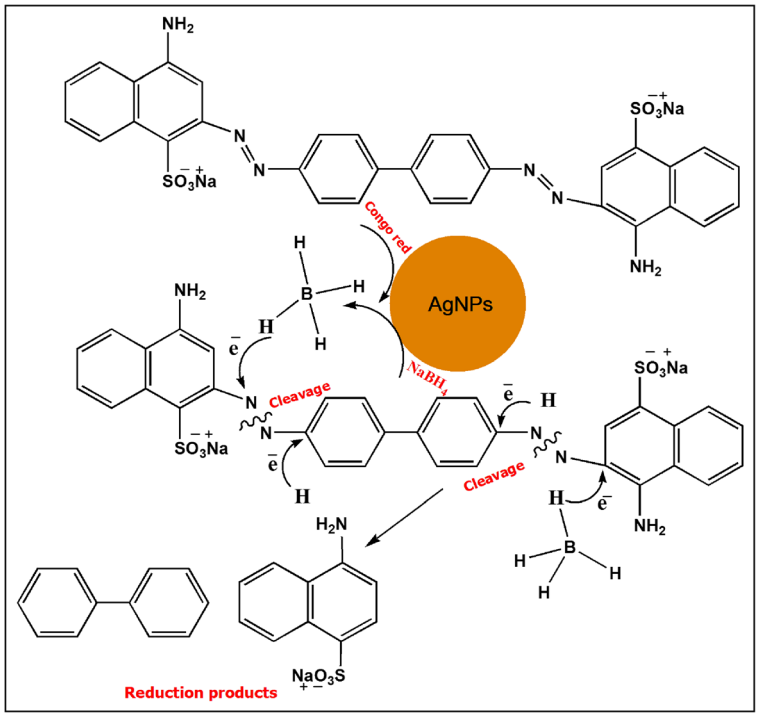

Scheme 1 Proposed mechanism of the catalytic reduction and degradation of CR dye by the synthesized AgNPs at room temperature

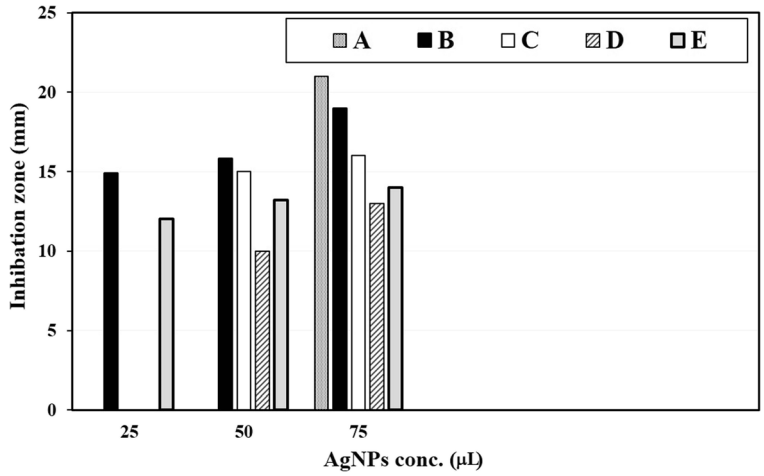

Fig. 9 Bacteria inhibition zone of different doses (25, 50, and 75 µL) of AgNPs (20Ag) where *A* (*Escherichia coli*), *B* (*Shigella* sp.). *C* (*Staphylococcus aureus*), *D* (*Salmonella typhi*) and *E* (*Pseudomonas aeruginosa*)

silver ions invade the bacterial cells and inhibit many cellular enzymes especially the respiratory chain enzymes via adhering to sulfur containing macromolecules leading to protein inhibition and death (Salar et al. 2015).

Conclusions

The present study represents an environmentally sound method for stable AgNPs synthesis from silver nitrate solution using accessible green marine algae (*C. serrulata*) aqueous extract. The impact of some synthesis conditions such as extract concentration, the contact time, pH values and temperature on the size of AgNPs was investigated and optimized. The results showed that AgNPs were formed during 24 h and the reduction rate of Ag ions was enhanced at higher temperature (95 °C) and higher pH values (>6.65). Moreover, TEM analysis reveal that higher extract concentration and higher temperature leading to the formation of crystalline, spherical AgNPs with an average particle size of 10 ± 2 nm. The catalytic results approve that the absence of AgNPs or $NaBH_4$ did not produce fading or bleaching for the CR color. Remarkably, upon addition of AgNPs into the mixture of CR and $NaBH_4$, fast reduction of CR occurs within 5 mins. Moreover, the catalytic degradation effectiveness of CR increases by increasing the extract concentration, $NaBH_4$ concentration, and catalyst dosage. Additionally, the synthesized AgNPs showed effective action against both gram negative and gram positive microscopic organisms. Due to the high degree of stability of the synthesized AgNPs and their excellent catalytic ability to degrade the most environmentally toxic dye (azo). This study reveals the possibility of producing highly efficient, stable, cost-effective, and easily recoverable catalyst employed for the elimination of toxic dyes and other pollutants from the environment. This could be possible via using the aqueous extract to synthesize AgNPs onto different solid surfaces such as silica, TiO_2, Fe_3O_4, carbon nanotubes, and graphene oxide. Hence, the AgNPs synthesized by the present strategy will discover promising applications in catalysis and wastewater treatment.

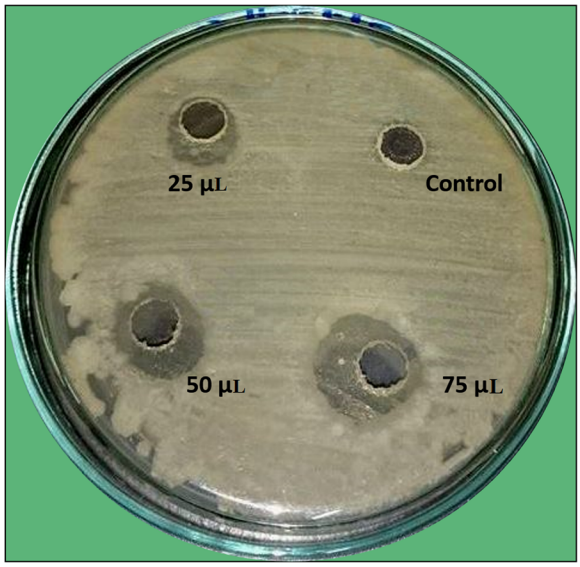

Fig. 10 Antibacterial test of different dosages (25, 50, and 75 µL) of AgNPs (20Ag) in a nutrient agar medium against *Shigella* sp.

References

Abbasi, E., Milani, M., Fekri Aval, S., Kouhi, M., Akbarzadeh, A., Tayefi Nasrabadi, H., Nikasa, P., Joo, S. W., Hanifehpour, Y., & Nejati-Koshki, K. (2016). Silver nanoparticles: synthesis methods, bio-applications and properties. *Critical Reviews in Microbiology, 42*, 173–180.

Aboubaraka, A. E., Aboelfetoh, E. F., & Ebeid, E.-Z. M. (2017). Coagulation effectiveness of graphene oxide for the removal of turbidity from raw surface water. *Chemosphere, 181*, 738–746.

Ahmed, S., Ahmad, M., Swami, B. L., & Ikram, S. (2016). A review on plants extract mediated synthesis of silver nanoparticles for antimicrobial applications: a green expertise. *Journal of Advanced Research, 7*, 17–28.

Ashokkumar, S., Ravi, S., Kathiravan, V., & Velmurugan, S. (2015). Synthesis of silver nanoparticles using *A. indicum* leaf extract and their antibacterial activity. *Spectrochimica Acta Part a: Molecular and Biomolecular Spectroscopy, 134*, 34–39.

Ayati, A., Ahmadpour, A., Bamoharram, F. F., Tanhaei, B., Mänttäri, M., & Sillanpää, M. (2014). A review on catalytic applications of Au/TiO 2 nanoparticles in the removal of water pollutant. *Chemosphere, 107*, 163–174.

Barbier, P., Guise, S., Huitorel, P., Amade, P., Pesando, D., Briand, C., & Peyrot, V. (2001). Caulerpenyne from *Caulerpa taxifolia* has an antiproliferative activity on tumor cell line SK-N-SH and modifies the microtubule network. *Life Sciences, 70*, 415–429.

Chen, M., Liu, P., Wang, C., Ren, W., & Diao, G. (2014). Fast catalytic reduction of an azo dye by recoverable and reusable Fe 3 O 4@ PANI@ Au magnetic composites. *New Journal of Chemistry, 38*, 4566–4573.

Ciavatta, M. L., Lopez Gresa, M. P., Gavagnin, M., Manzo, E., Mollo, E., D'Souza, L., & Cimino, G. (2006). New caulerpenyne-derived metabolites of an Elysia Sacoglossan from the south Indian coast. *Molecules, 11*, 808–816.

De Gaillande, C., Payri, C., Remoissenet, G., & Zubia, M. (2016). Caulerpa consumption, nutritional value and farming in the Indo-Pacific region. *Journal of Applied Phycology*, 1–18. doi:10.1007/s10811-016-0912-6.

Dong, C., Cao, C., Zhang, X., Zhan, Y., Wang, X., Yang, X., Zhou, K., Xiao, X., & Yuan, B. (2017). Wolfberry fruit (*Lycium barbarum*) extract mediated novel route for the green synthesis of silver nanoparticles. *Optik-International Journal for Light and Electron Optics, 130*, 162–170.

Dumay, O., Pergent, G., Pergent-Martini, C., & Amade, P. (2002). Variations in caulerpenyne contents in *Caulerpa taxifolia* and *Caulerpa racemosa*. *Journal of Chemical Ecology, 28*, 343–352.

Edison, T. N. J. I., Atchudan, R., Kamal, C., & Lee, Y. R. (2016a). *Caulerpa racemosa*: a marine green alga for eco-friendly synthesis of silver nanoparticles and its catalytic degradation of methylene blue. *Bioprocess and Biosystems Engineering, 39*, 1401–1408.

Edison, T. N. J. I., Lee, Y. R., & Sethuraman, M. G. (2016b). Green synthesis of silver nanoparticles using Terminalia cuneata and its catalytic action in reduction of direct yellow-12 dye. *Spectrochimica Acta Part A: Molecular and Biomolecular Spectroscopy, 161*, 122–129.

El-Kassas, H. Y., & Ghobrial, M. G. (2017). Biosynthesis of metal nanoparticles using three marine plant species: anti-algal efficiencies against "Oscillatoria Simplicissima". *Environmental Science and Pollution Research, 24*, 7837–7849.

Fawcett, D., Verduin, J.J., Shah, M., Sharma, S.B., Poinern, G.E.J., 2017. A Review of Current Research into the Biogenic Synthesis of Metal and Metal Oxide Nanoparticles via Marine Algae and Seagrasses. *Journal of Nanoscience* 2017.

Fischel, J., Lemee, R., Formento, P., Caldani, C., Moll, J., Pesando, D., Meinesz, A., Grelier, P., Pietra, P., & Guerriero, A. (1994). Cell growth inhibitory effects of caulerpenyne, a sesquiterpenoid from the marine algae *Caulerpa taxifolia*. *Anticancer Research, 15*, 2155–2160.

Gabriel, J. S., Gonzaga, V. A., Poli, A. L., & Schmitt, C. C. (2017). Photochemical synthesis of silver nanoparticleson chitosans/montmorillonite nanocomposite films and antibacterial activity. *Carbohydrate Polymers, 171*, 202–210.

Ganapuram, B. R., Alle, M., Dadigala, R., Dasari, A., Maragoni, V., & Guttena, V. (2015). Catalytic reduction of methylene blue and Congo red dyes using green synthesized gold nanoparticles capped by salmalia malabarica gum. *International Nano Letters, 5*, 215–222.

Gangula, A., Podila, R., Karanam, L., Janardhana, C., & Rao, A. M. (2011). Catalytic reduction of 4-nitrophenol using biogenic gold and silver nanoparticles derived from Breynia rhamnoides. *Langmuir, 27*, 15268–15274.

Garcia, J. C., de Souza Freitas, T. K. F., Palácio, S. M., Ambrósio, E., Souza, M. T. F., Santos, L. B., de Cinque Almeida, V., & de Souza, N. E. (2013). Toxicity assessment of textile effluents treated by advanced oxidative process (UV/TiO2 and UV/TiO2/H2O2) in the species *Artemia salina* L. *Environmental Monitoring and Assessment, 185*, 2179–2187.

Gemeay, A. H., Elsharkawy, R. G., Aboelfetoh, E. F. (2017). Graphene Oxide/Polyaniline/Manganese Oxide Ternary Nanocomposites, Facile Synthesis, Characterization, and Application for Indigo Carmine Removal. *Journal of Polymers and the Environment*, 1–15. doi:10.1007/s10924-017-0947-z.

Ghosh, B. K., Hazra, S., Naik, B., & Ghosh, N. N. (2015). Preparation of Cu nanoparticle loaded SBA-15 and their excellent catalytic activity in reduction of variety of dyes. *Powder Technology, 269*, 371–378.

González-Ballesteros, N., Prado-López, S., Rodríguez-González, J., Lastra, M., & Rodríguez-Argüelles, M. (2017). Green synthesis of gold nanoparticles using brown algae *Cystoseira baccata*: Its activity in colon cancer cells. *Colloids and Surfaces B: Biointerfaces, 153*, 190–198.

Gurusamy, V., Krishnamoorthy, R., Gopal, B., & Veeraravagan, V. (2017). Systematic investigation on hydrazine hydrate assisted reduction of silver nanoparticles and its antibacterial properties. *Inorganic and Nano-Metal Chemistry, 47*, 761–767.

Ibrahim, H. M. (2015). Green synthesis and characterization of silver nanoparticles using banana peel extract and their antimicrobial activity against representative microorganisms. *Journal of Radiation Research and Applied Sciences, 8*, 265–275.

Indana, M. K., Gangapuram, B. R., Dadigala, R., Bandi, R., & Guttena, V. (2016). A novel green synthesis and characterization of silver nanoparticles using gum tragacanth and evaluation of their potential catalytic reduction activities with methylene blue and Congo red dyes. *Journal of Analytical Science and Technology, 7*, 19.

Kamal, T., Khan, S. B., & Asiri, A. M. (2016). Synthesis of zero-valent cu nanoparticles in the chitosan coating layer on cellulose microfibers: evaluation of azo dyes catalytic reduction. *Cellulose, 23*, 1911–1923.

Kathiraven, T., Sundaramanickam, A., Shanmugam, N., & Balasubramanian, T. (2015). Green synthesis of silver nanoparticles using marine algae *Caulerpa racemosa* and their antibacterial activity against some human pathogens. *Applied Nanoscience, 5*, 499–504.

Khalil, M. M., Ismail, E. H., El-Baghdady, K. Z., & Mohamed, D. (2014). Green synthesis of silver nanoparticles using olive leaf extract and its antibacterial activity. *Arabian Journal of Chemistry, 7*, 1131–1139.

Khan, Z., Al-Thabaiti, S. A., Obaid, A. Y., & Al-Youbi, A. (2011). Preparation and characterization of silver nanoparticles by chemical reduction method. *Colloids and Surfaces B: Biointerfaces, 82*, 513–517.

Khodadadi, B., Bordbar, M., Yeganeh-Faal, A., & Nasrollahzadeh, M. (2017). Green synthesis of Ag nanoparticles/clinoptilolite using Vacciniummacrocarpon fruit extract and its excellent catalytic activity for reduction of organic dyes. *Journal of Alloys and Compounds, 719*, 82–88.

Khodashenas, B., & Ghorbani, H. R. (2015). Synthesis of silver nanoparticles with different shapes. *Arabian Journal of Chemistry*. doi:10.1016/j.arabjc.2014.12.014.

Kim, S.-K. (2011). *Handbook of marine macroalgae: biotechnology and applied phycology*. Chichester: Wiley.

Liu, X., & Astruc, D. (2017). From Galvanic to Anti-Galvanic Synthesis of Bimetallic Nanoparticles and Applications in Catalysis, Sensing, and Materials Science. *Advanced Materials* 29. doi:10.1002/adma.201605305.

Liu, W., Herrmann, A.-K., Bigall, N. C., Rodriguez, P., Wen, D., Oezaslan, M., Schmidt, T. J., Gaponik, N., & Eychmüller, A. (2015). Noble metal aerogels synthesis, characterization, and application as electrocatalysts. *Accounts of Chemical Research, 48*, 154–162.

Liu, K.-G., Abbasi, A. R., Azadbakht, A., Hu, M.-L., & Morsali, A. (2017a). Deposition of silver nanoparticles on polyester fiber under ultrasound irradiations. *Ultrasonics Sonochemistry, 34*, 13–18.

Liu, X., Iocozzia, J., Wang, Y., Cui, X., Chen, Y., Zhao, S., et al. (2017b). Noble metal–metal oxide nanohybrids with tailored nanostructures for efficient solar energy conversion, photocatalysis and environmental remediation. *Energy & Environmental Science, 10*, 402–434.

Loo, Y. Y., Chieng, B. W., Nishibuchi, M., & Radu, S. (2012). Synthesis of silver nanoparticles by using tea leaf extract from *Camellia sinensis*. *International Journal of Nanomedicine, 7*, 4263.

Mahmudin, L., Suharyadi, E., Utomo, A. B. S., & Abraha, K. (2015). Optical properties of silver nanoparticles for surface plasmon resonance (SPR)-based biosensor applications. *Journal of Modern Physics, 6*.

Makarov, V., Love, A., Sinitsyna, O., Makarova, S., Yaminsky, I., Taliansky, M., Kalinina, N., 2014. "Green" nanotechnologies: synthesis of metal nanoparticles using plants. *Acta Naturae (англоязычная версия)* 6.

Marić, P., Ahel, M., Senta, I., Terzić, S., Mikac, I., Žuljević, A., & Smital, T. (2017). Effect-directed analysis reveals inhibition of zebrafish uptake transporter Oatp1d1 by caulerpenyne, a major secondary metabolite from the invasive marine alga *Caulerpa taxifolia*. *Chemosphere, 174*, 643–654.

Nadaf, N. Y., & Kanase, S. S. (2016). Biosynthesis of gold nanoparticles by Bacillus marisflavi and its potential in catalytic dye degradation. *Arabian Journal of Chemistry*. doi:10.1016/j.arabjc.2016.09.020.

Nagappan, T., & Vairappan, C. S. (2014). Nutritional and bioactive properties of three edible species of green algae, genus Caulerpa (Caulerpaceae). *Journal of Applied Phycology, 26*, 1019–1027.

Narayanan, K. B., Park, H. H., & Han, S. S. (2015). Synthesis and characterization of biomatrixed-gold nanoparticles by the mushroom Flammulina velutipes and its heterogeneous catalytic potential. *Chemosphere, 141*, 169–175.

Nasrollahzadeh, M., Atarod, M., Jaleh, B., & Gandomirouzbahani, M. (2016). In situ green synthesis of ag nanoparticles on graphene oxide/TiO 2 nanocomposite and their catalytic activity for the reduction of 4-nitrophenol, congo red and methylene blue. *Ceramics International, 42*, 8587–8596.

Nesic, A. R., Kokunesoski, M. J., Volkov-Husovic, T. D., & Velickovic, S. J. (2016). New method for quantification of dye sorption using SBA mesoporous silica as a target sorbent. *Environmental Monitoring and Assessment, 188*, 1–12.

Ngo, Y. H., Li, D., Simon, G. P., & Garnier, G. (2012). Gold nanoparticle–paper as a three-dimensional surface enhanced raman scattering substrate. *Langmuir, 28*, 8782–8790.

Pal, A., Shah, S., & Devi, S. (2009). Microwave-assisted synthesis of silver nanoparticles using ethanol as a reducing agent. *Materials Chemistry and Physics, 114*, 530–532.

Pandey, S., Ramontja, J., 2016. Turning to nanotechnology for water pollution control: applications of nanocomposites. *Focus on Sciences* 2.

Philip, D. (2010). Honey mediated green synthesis of silver nanoparticles. *Spectrochimica Acta Part A: Molecular and Biomolecular Spectroscopy, 75*, 1078–1081.

Pretsch, E., Bühlmann, P., Affolter, C., Pretsch, E., Bhuhlmann, P., & Affolter, C. (2009). *Structure determination of organic compounds* (vol 13). Berlin: Springer.

Priyadarshini, E., Pradhan, N., Sukla, L.B., Panda, P.K., 2014. Controlled synthesis of gold nanoparticles using aspergillus terreus IF0 and its antibacterial potential against gram negative pathogenic bacteria. *Journal of Nanotechnology* 2014.

Rajabi, H.R., Naghiha, A., Kheirizdeh, M., Sadatfaraji, H., Mirzaei, A., & Alvand, Z. M. (2017). Microwave assisted extraction as an efficient approach for biosynthesis of zinc oxide nanoparticles: synthesis, characterization, and biological properties. *Materials Science and Engineering: C, 78*, 1109–1118.

Rajakumar, G., & Rahuman, A. A. (2016). *Phytosynthesis of metal and metal-oxide nanoparticles–technological concepts and their biomedical applications, nanoparticles in the fight against parasites* (pp. 51–80). Switzerland: Springer.

Ren, M., Jin, Y., Chen, W., & Huang, W. (2015). Rich capping ligand–ag colloid interactions. *The Journal of Physical Chemistry C, 119*, 27588–27593.

Salar, R. K., Sharma, P., & Kumar, N. (2015). Enhanced antibacterial activity of streptomycin against some human pathogens using green synthesized silver nanoparticles. *Resource-Efficient Technologies, 1*, 106–115.

Saratale, R. G., Saratale, G., Chang, J., & Govindwar, S. (2011). Bacterial decolorization and degradation of azo dyes: a review. *Journal of the Taiwan Institute of Chemical Engineers, 42*, 138–157.

Sfecci, E., Le Quemener, C., Lacour, T., Massi, L., Amade, P., Audo, G., et al. (2017). Caulerpenyne from *Caulerpa taxifolia*: a comparative study between CPC and classical chromatographic techniques. *Phytochemistry Letters, 81*, 557. doi:10.1055/s-0036-1596624.

Shah, L. A., Haleem, A., Sayed, M., & Siddiq, M. (2016). Synthesis of sensitive hybrid polymer microgels for catalytic reduction of organic pollutants. *Journal of Environmental Chemical Engineering, 4*, 3492–3497.

Siddiqui, M. N., Redhwi, H. H., Achilias, D. S., Kosmidou, E., Vakalopoulou, E., Ioannidou, M.D. (2017). Green synthesis of silver nanoparticles and study of their antimicrobial properties. *Journal of Polymers and the Environment*, 1–11. doi:10.1007/s10924-017-0962-0.

Sreekanth, T., Jung, M.-J., & Eom, I.-Y. (2016). Green synthesis of silver nanoparticles, decorated on graphene oxide nanosheets and their catalytic activity. *Applied Surface Science, 361*, 102–106.

Tiwari, N. R., Rathore, A., Prabhune, A., & Kulkarni, S. K. (2010). Gold nanoparticles for colorimetric detection of hydrolysis of antibiotics by penicillin G acylase. *Advances in Bioscience and Biotechnology, 1*, 322.

Velammal, S. P., Devi, T. A., & Amaladhas, T. P. (2016). Antioxidant, antimicrobial and cytotoxic activities of silver and gold nanoparticles synthesized using *Plumbago zeylanica* bark. *Journal of Nanostructure in Chemistry, 6*, 247–260.

Verma, S., Rao, B. T., Srivastava, A., Srivastava, D., Kaul, R., & Singh, B. (2017). A facile synthesis of broad plasmon wavelength tunable silver nanoparticles in citrate aqueous solutions by laser ablation and light irradiation. *Colloids and Surfaces a: Physicochemical and Engineering Aspects, 527*, 23–33.

Vidhu, V., & Philip, D. (2014). Catalytic degradation of organic dyes using biosynthesized silver nanoparticles. *Micron, 56*, 54–62.

Wang, L., Li, J., Wang, Z., Zhao, L., & Jiang, Q. (2013). Low-temperature hydrothermal synthesis of α-Fe/Fe 3 O 4 nanocomposite for fast Congo red removal. *Dalton Transactions, 42*, 2572–2579.

Wang, H., Wang, H., Li, T., Ma, J., Li, K., & Zuo, X. (2017). Silver nanoparticles selectively deposited on graphene-colloidal carbon sphere composites and their application for hydrogen peroxide sensing. *Sensors and Actuators B: Chemical, 239*, 1205–1212.

Wells, M. L., Potin, P., Craigie, J. S., Raven, J. A., Merchant, S. S., Helliwell, K. E., et al. (2016). Algae as nutritional and functional food sources: revisiting our understanding. *Journal of Applied Phycology, 29*, 949–982.

Yian Zheng, A. W. (2012). Ag nanoparticle-entrapped hydrogel as promising material for catalytic reduction of organic dyes. *Journal of Materials Chemistry, 22*, 16552–16559.

Zhang, J., Chaker, M., & Ma, D. (2017). Pulsed laser ablation based synthesis of colloidal metal nanoparticles for catalytic applications. *Journal of Colloid and Interface Science, 489*, 138–149.